An original experimental approach showing that most nonlinearities expressed by filled elastomers relate to microscopic friction and cavitation

Marion Picquart, Gilles Poirey, Guillaume Puel, D. Aubry

An original experimental approach to investigate the role of friction and cavitation on the nonlinear behavior of filled elastomers

M. PICQUART[1,2], G. POIREY[1], G. PUEL[2], D. AUBRY[2]

1. ArianeGroup, 9 rue Lavoisier, CRB, 91710 Vert-le-Petit, France

2. MSSMat laboratory (CentraleSupélec / CNRS UMR 8579 / Paris-Saclay University), 3 rue Joliot Curie, 91190 Gif-sur-Yvette, France

Dated: April 11, 2020

ABSTRACT: Filled elastomers present a highly nonlinear behavior when submitted to cyclic mechanical loads. Origins of these nonlinearities are still uncertain, but many models are based on micromechanisms such as friction or cavitation at the filler/binder interface. To substantiate these hypotheses, an experimental approach is proposed to assess the real effects of friction and cavitation on the macroscopic response. HTPB, a linear, viscoelastic, transparent material, is used to create macroscopic samples in which mechanisms are activated, separately or jointly. Responses of these samples allow to point out the shapes and amplitudes of the nonlinearities generated by each mechanism. A deeper analysis of the resulting curves allows to correlate the nonlinearities characteristics to the ones expressed by filled elastomers, therefore consolidate the basis of future models.

Keywords: Filled Elastomers; Viscoelasticity; Nonlinearities; Micromechanisms; Friction; Cavitation

INTRODUCTION

From carbon-black reinforced natural rubbers to elastomeric binders full of energetic particles, filled elastomers are widely used in the industry. Their viscoelastic, highly nonlinear behavior under cyclic mechanical loads, is well known and documented, but the actual sources of these nonlinearities are still unclear. Many theories are proposed, but none of them meets with general agreement[2].

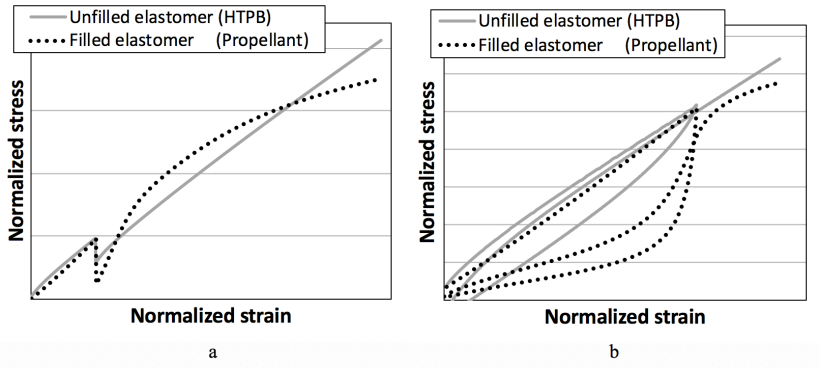

Figure 1: Comparison between the linear response of an unfilled elastomer and the nonlinear response of a filled elastomer to unitary loading-relaxation (a) and loading-unloading (b) cycles.

Unfilled elastomers present time, pressure and strain dependent properties, express a linear viscoelastic behavior and can sustain several thousands of percent of strain. When reinforced with particles, their stiffness increases, breakage occurs earlie (for a few tens of percent of strain) and they express a strongly nonlinear behavior[1]. Figure 1 compares the response of an unfilled elastomer (Hydroxyl-Terminated Polybutadiene) and a filled elastomer (study propellant) to two cyclic mechanical loads: a loading-relaxation and a loading-unloading; more detailed list of nonlinearities is available in Appendix . Thus, the question is to determine what creates such a difference between the behaviors of filled and unfilled elastomers.

Many theories have been advanced regarding the nonlinearities origins, especially the Mullins' effect[2]. The role played by the micro-component morphology and chemical nature is often questioned and has been the object of different studies[3–6]. Despite the undeni-

able influence of the microstructure composition on the macroscopic mechanical properties, the fact that all filled elastomers express similar nonlinearities[4–10] directs towards common mechanisms.

Elastomeric chains behavior like elongation[11], breakage[7] and disentanglement[8], as well as network cross-links breakage[12] are also considered. But nonlinearities taking their source only in the binder behavior seems unlikely, because these mechanisms also occur inside unfilled elastomers, that, apart from rubbers presenting stress-induced crystallization[2], behave linearly.

Micromechanisms related to binder/fillers interactions seem more likely. Particles presence induces high strain and stress concentrations in the microstructure, leading to filler-binder interface breakage[13,14]. Once the interface is broken, the binder can move off the particle, or slide along it, depending on the local stress state. Cavitation is the most frequently used mechanism to build nonlinear models[9,10,13,15,16]. Microscopic observations[17], or macroscopic dilatation measures[18] are evidences of the voids presence. Nonlinearities expressed under simple shear tests[15,19], that prevent micro-cavitation, indicate the involvement of another mechanism. This could be explained by filler/binder friction, which is also used in some model developments[20–22]. To the authors knowledge, no current model accounts for both mechanisms simultaneously.

None of the above references provides detailed investigations on the direct effect of friction and cavitation on the macroscopic nonlinearities. In situ observations of the microstructure during cyclic loadings are possible, by means of advanced experimental resources like nuclear magnetic resonance spectroscopy[23] or digital volume correlation[14], but they do not permit to isolate the mechanisms.

This study offers to evaluate the real impact of friction and cavitation, as separated mechanisms, on the macroscopic response of filled elastomers. The idea is to ensure that their activation generates nonlinearities similar to the ones expressed by filled elastomers. A new experimental approach is proposed, with macorsocpic samples submitted to cyclic mechanical loads; a filled elastomer (propellant) is also submitted to similar experiments for comparison.

EXPERIMENTS

To ease results interpretation, the proposed experimental set up meets the following requirements: mechanisms are dissociated to allow separate investigation, and mechanisms occurrence can be ensured without the need for microscopic devices.

Material selection

The idea is to introduce the studied mechanisms into a material known no behave linearly, so as to notice first-hand the activation of some nonlinearities. Hydroxyl-Terminated Polybutadiene (HTPB) is an amorphous elastomer used as a binder in several solid propellants. As already shown on Figure 1, it expresses a viscoelastic linear behavior. Produced in a liquid state, it requires 15 days of curing to gain stiffness. It contains only 30% of plasticizer, which makes it easy to bond to metallic parts. Moreover, its transparency is a non-negligible asset, as it allows a direct observation of everything happening inside the sample. HTPB seems to be the ideal candidate for this study. For reasons of confidentiality, the exact composition cannot be disclosed.

Samples design

Four macroscopic geometries are designed: one for reference, one for cavitation only, one for friction only and one for both friction and cavitation. Dimensions are presented on Figure 2.

- Reference samples are homogeneous: they are only composed of unfilled HTPB, so they express a linear behavior. They present a 20 mm diameter and a 18 mm effective length.
- Friction samples present the same geometry, in addition to a 15 mm diameter central channel. To create the channel, a specific cylindrical part is added inside the mold, and removed from the sample after curing. A metallic bar is introduced in the channel before the experiment; friction is activated when the sample is stretched and HTPB slides in contact with the metal.

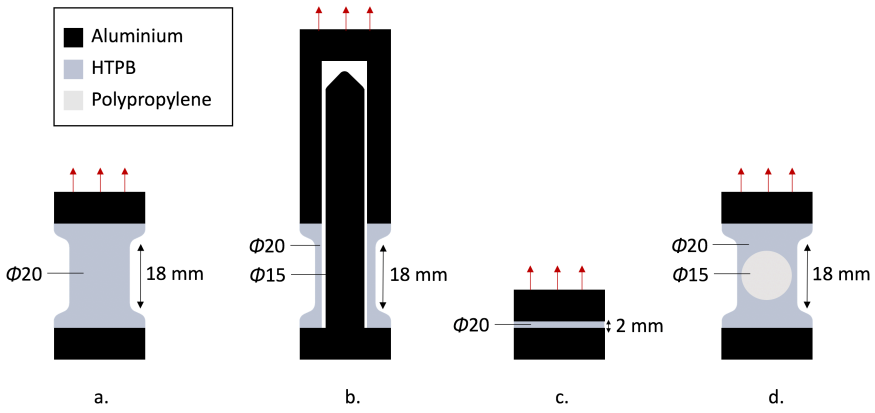

Figure 2: Dimensions of the reference (a), friction (b), cavitation (c), and inclusion (d) samples. Aluminum end-plates attaching the sample to the test machine are represented in black.

- Cavitation samples are 20 mm diameter, 2 mm height HTPB discs. This geometry is usually used to find the material cavitation limit[24]: because it is incompressible, the material cannot sustain a triaxial state of stress and voids appear inside the sample. Comparing the response of this sample to cyclic loads before, and after this cavitation limit will permit to study this mechanism influence.

- Inclusion samples are more representative of the propellant microstructure. They are composed of a 15 mm diameter Polypropylene ball, representing a propellant filler, embedded in HTPB; the stiffness difference between Polypropylene (100 MPa) and HTPB (1 MPa) is typical of real propellant components, and so is the spherical shape, more representative than a cylinder. Plastic was chosen over metal for processing reasons. Stress concentrations around the particles lead to an interface breakage, activating cavitation and friction. Introducing macroscopic balls inside samples has been made during a study on adhesive properties[25].

Samples manufacturing

Reference, friction, and inclusion samples are made by pouring HTPB into specific molds and cured for 15 days at 50 °C. Inclusion samples require a two-times curing to set the inclusion at the right place: a first half of the mold is filled with HTPB in liquid state,

Figure 3: Photographies of the reference (a), friction (b), cavitation (cast between two end-plates) (c), and inclusion (d) samples after unmolding.

and the inclusion is positioned using a special centralizer. After one day of curing, the inclusion is embedded in partially reticulated HTPB; the centralizer is removed, and the mold is filled with a new preparation of HTPB. Samples are then cooked for 15 days at 50 °C. Complementary experiments have been conducted to ensure this double curing has no significant influence on the mechanical response, nor on the breakage location. Cavitation samples are cut out from HTPB plates of 2 mm thickness, also cured for 15 days at 50 °C. This fabrication process is precise and makes the samples very reproductible (Figure 3).

Experimental campaign

Different cyclic loads are applied to the samples. All experiments are conducted at room temperature, at a constant strain rate of 0.05 s^{-1} and up to breakage. A new sample is used for each test.

- Monotonous tensile test, with a constant deformation rate applied until breakage.
- Successive loading-unloading$_1$ cyclic tests, with a strain level increase of 10% between each cycle. Unloading steps stop when a force of zero Newton is reached, to avoid samples compression and buckling.
- Successive loading-unloading$_5$ cyclic tests, with 5-cycle series up to the same strain level, starting every 50% of strain.
- Successive loading-relaxation cyclic tests, with a strain level increase of 10% between each cycle. Relaxations (strain maintained constant) last ten times longer than one

loading step.

Each experiment is conducted at least twice and presents a good repeatability.

RESULTS

Images and curves collected from the experiments are presented in this part. They confirm the activation of the mechanisms and show their important effect on the samples response.

Visual validation

Metallic end-plates are bound to the samples using bi-component polyurethane and attached to the machine cross-head using immediate-hardening cyanoacrylate. A circular LED lighting (OPT Machine Vison, 150 mm diameter) composed of tilted cold diodes is placed behind the samples, and the HTPB transparency allows to visualize mechanisms occurring inside the material. The testing machine is a Shimadzu AGS-X Series with a translating upper cross head. Some images are registered during the experiments at a rate of 60 images per second, using a Canon 60D camera with a Sigma 150 mm f2.8 Macro lens. Some sequences show interesting results.

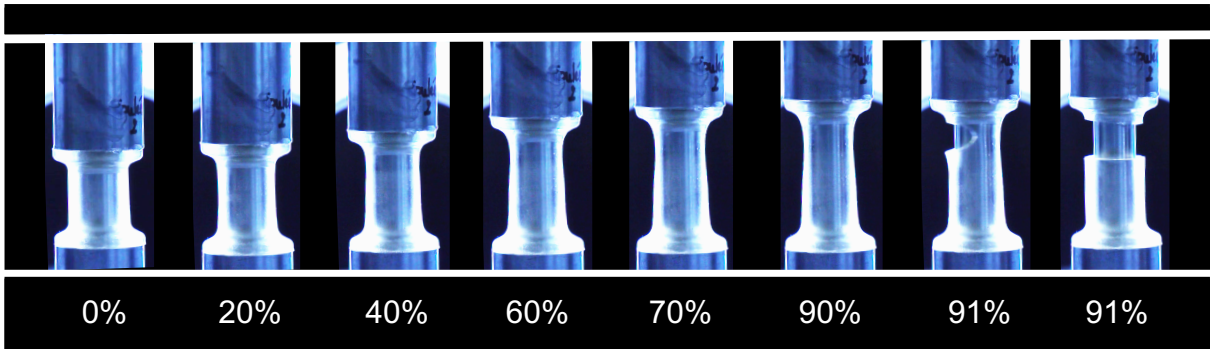

Figure 4: Sequence registered during a monotonous tensile test on a friction sample at different strain levels.

Figure 4 shows the evolution of a friction sample during a monotonous tensile test. The stillness of the metallic bar (inside the sample) and of the lower cross-head explains the induced asymmetry. From 60% of strain, an important shrinkage is visible at the top of

the sample, which confirms the activation of friction. Eventually this shrinkage leads to the sample breakage.

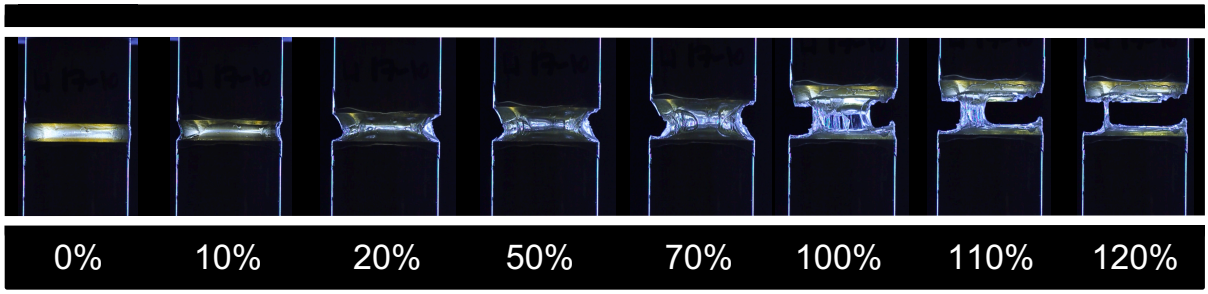

Figure 5: Sequence registered during a monotonous tensile test on a cavitation sample at different strain levels.

Figure 5 shows the evolution of a cavitation sample during a monotonous tensile test. The meniscus appearing near the edges at 10% of strain indicates that the stress state is not completely hydrostatic. However, the area sustaining a triaxial loading is large enough to generate cavitation. At 20% of strain, cavities start to appear inside the material. From 70% of strain, cavities coalesce, eventually leading to the sample breakage.

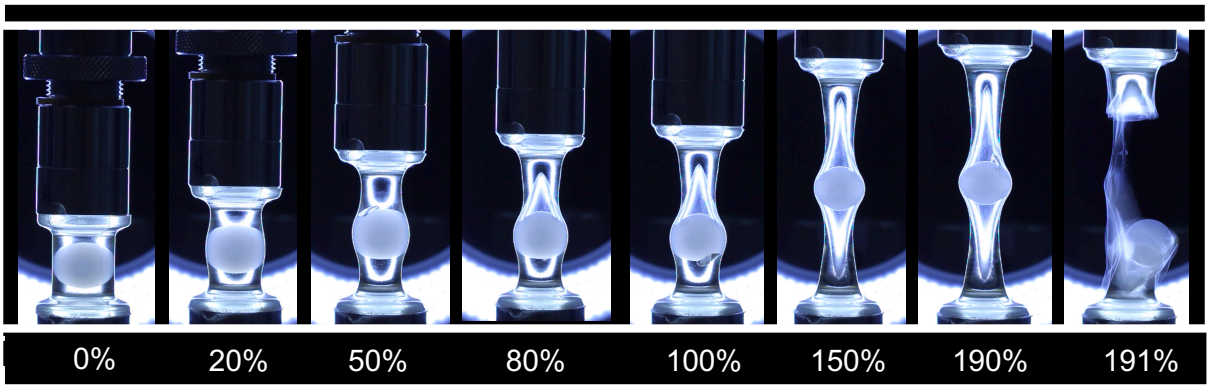

Figure 6: Sequence registered during a monotonous tensile test on an inclusion sample at different strain levels.

Figure 6 shows the evolution of an inclusion sample during a monotonous tensile test. At 50% of strain, a small void appears at the top of the Polypropylene ball, instantly followed by a larger debonding. At 100% of strain, a similar cavity appears at the bottom of the ball. The HTPB layer surrounding the polypropylene ball is very thin; a closer analysis of the

films showed a relative displacement of HTPB from the ball. This confirms the activation of friction. Around 190% of strain, a crack appears, leading to the sample breakage. The voids creation is very sudden and dissipates energy, making it easy to identify on the stress curves.

Samples responses to cyclic loads

Cross head displacement and cell force measure are registered during each test. Since strain and stress fields are heterogeneous in the samples, initial sections are assumed to remain constant, and dilatation is neglected. Nominal stress versus logarithmic strain curves are plotted. Propellant signals are included for comparison; curves are gathered in Figure 7.

Results for the reference tests show the linear behavior of unfilled HTPB. Friction samples responses present a hysteretic behavior during unloading steps, together with a slope change. Large stress relaxations are also visible during loading-relaxation tests. Friction samples do not express Mullins' effect. The cavitation samples behavior also presents nonlinearities, although the trends are quite different. Before cavitation, the response is elastic, which is expected from an incompressible material undergoing a triaxial stress state. Right after first voids appearance, large amplitude hysteresis (unloadings) and stress losses (relaxations) are visible, and Mullins' effect is clearly recognizable. Contrary to the propellant case, unloading slopes are concave. The inclusion sample presents a combination of the nonlinearities mentioned above. The two cavitation times are identified by the two sudden stress decreases. The hysteretic behavior and Mullins' effect are visible, and amplified after cavitation, and so are the stress relaxations. Eventually, propellant curves are presented.

Figure 7 highlights a progressiveness of the nonlinearities from the unfilled elastomer linear behavior to the highly nonlinear behavior of the filled elastomer. It also shows that friction and cavitation are both responsible for nonlinearities, with very distinct amplitudes and shapes. This speaks in favor of a mechanisms combination in the filled elastomers microstructure. In the next part, results analysis is pushed further to correlate the friction and cavitation induced nonlinearities with the ones expressed by filled elastomers.

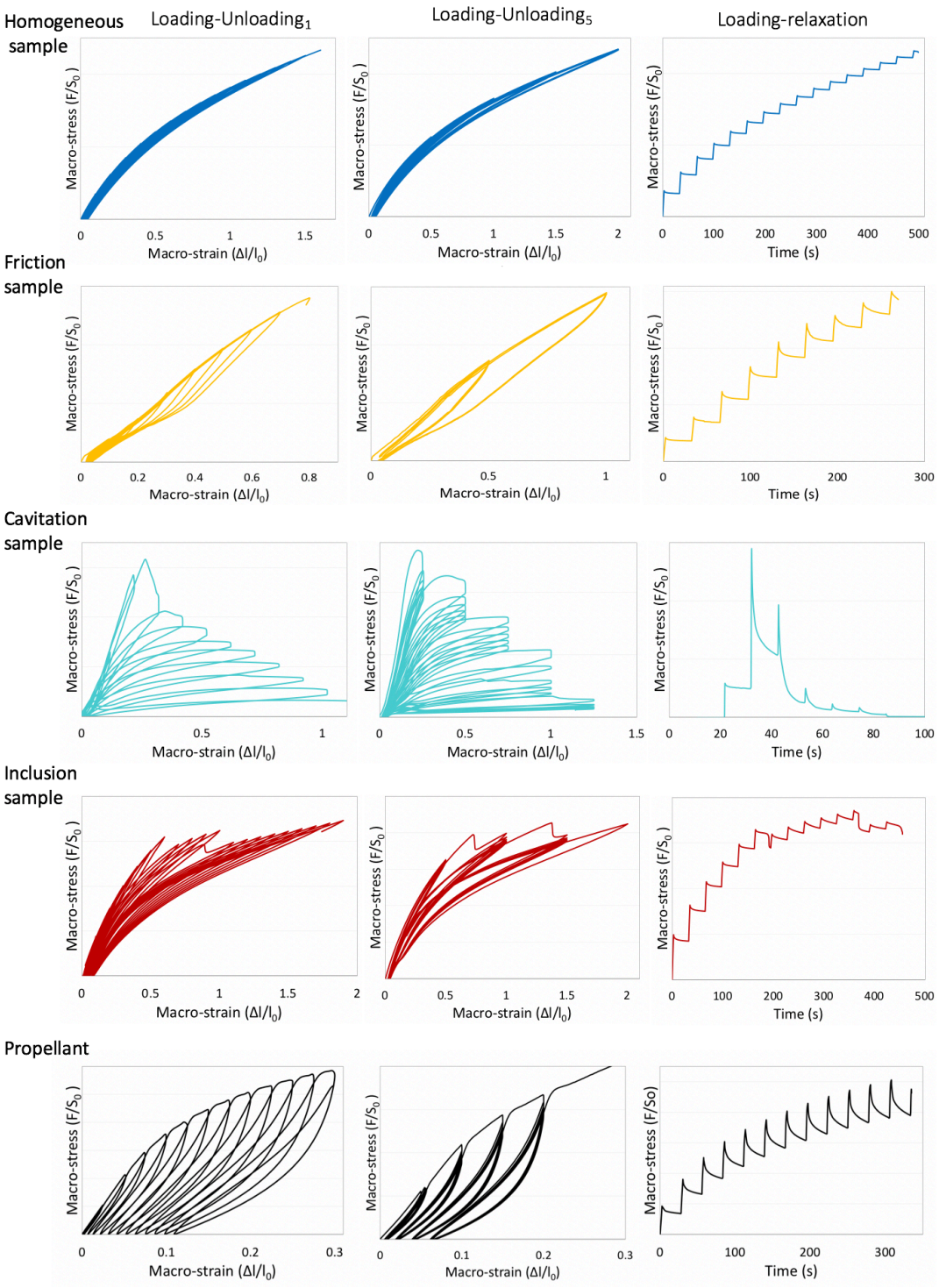

Figure 7: Responses of all HTPB samples to loading-unloading$_1$, loading-unloading$_5$ and loading-relaxation tests. Propellant responses are added for comparison.

Post-processing for a better insight into the mechanisms role

Two quantities are extracted from the stress curves: the dissipated energy and the reloading stiffness. Calculation methods are detailed on Appendix . For each sample, the strain level reached at each cycle corresponds to a same percentage of the final breakage strain, so, all curves can be presented on the same figure. These exploitations allow a closer comparison of the four samples responses with the propellant behavior.

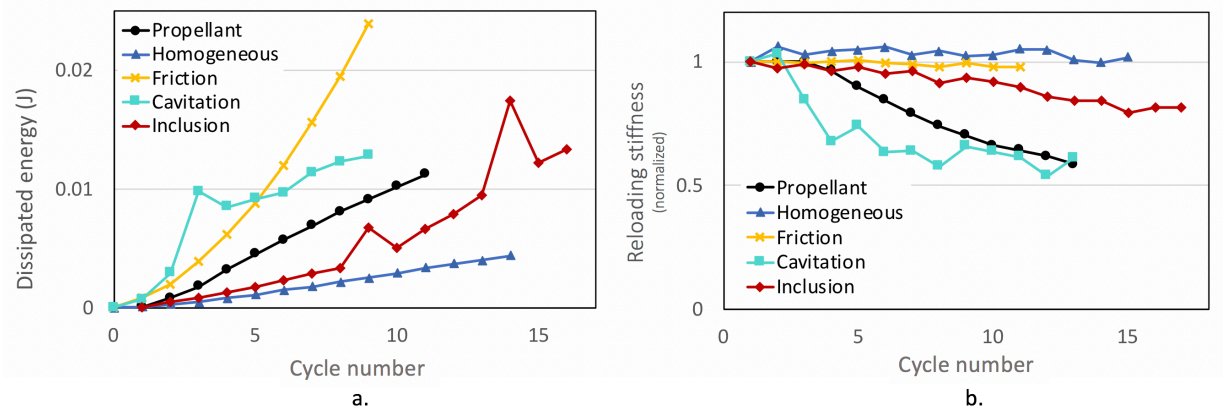

Figure 8: Comparison of the dissipated energy (a) and reloading stiffness (b) evolutions in propellant and HTPB samples, during loading-unloading$_1$ tests.

Figure 8a shows that the dissipation in the reference sample increases linearly. The increase is faster for propellant, friction and cavitation samples. The inclusion sample behavior is quite interesting, as it is very close to the reference sample until first cavitation at cycle 9. From this point, dissipation increases with a new slope, similar to the propellant one. This graph indicates that the evolution of the cycles amplitude of filled elastomers during loading-unloading$_1$ tests is due to both friction and cavitation. The loading stiffness evolution (Figure 8b) shows that friction behaves linearly as the curve remains constant like the reference one. Inclusion curve decreases slightly, and cavitation curve decreases strongly. Thus, the reloading stiffness evolution in the filled elastomers response is probably due to cavitation.

Figure 9a shows that friction does not take part to the stress softening occurring after each first cycle of the 5-cycle series (no Mullins' effect), contrary to cavitation and inclusion samples that behave like propellant: the large increase of dissipation at each strain increment,

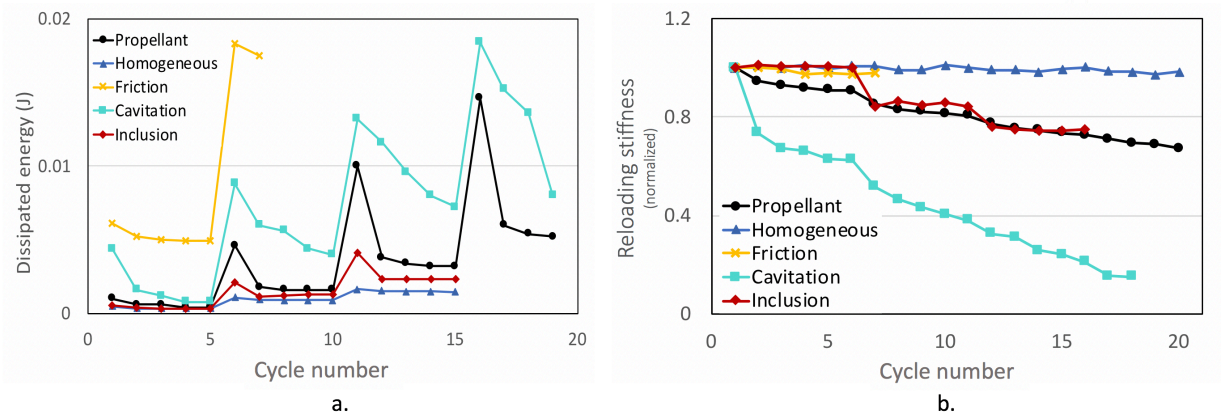

Figure 9: Comparison of the dissipated energy (a) and reloading stiffness (b) evolutions in propellant and HTPB samples, during loading-unloading$_5$ tests.

followed by a severe decrease for the four following cycles, is very clear. The Mullins' effect can be attributed to cavitation. It is reminded that Figure 7 showed the convesity of unloading curves is due to friction. Once again, the the reloading stiffness (Figure 9b) for friction remains constant whereas cavitation decreases strongly. Inclusion sample expresses a linear behavior before first cavitation and very similar to propellant after cavitation. Reloading stiffness evolution is attributed to cavitation again.

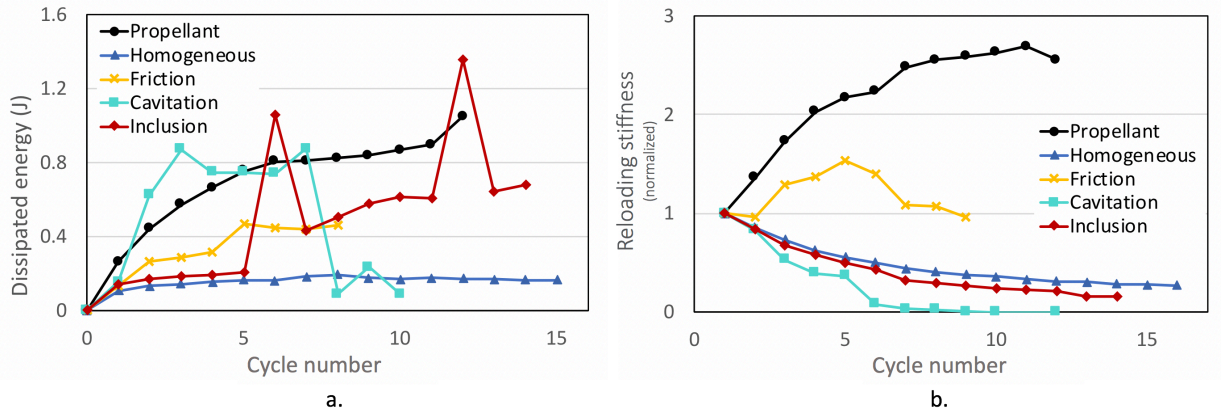

Figure 10: Comparison of the dissipated energy (a) and reloading stiffness (b) evolutions in propellant and HTPB samples, during loading-relaxation tests.

According to Figure 10a, stress relaxation amplitude remains constant in the reference case. Cavitation sample does not present stress relaxation before voids creation, at cycle

2. Friction sample also presents an increasing relaxation trend. Again, the inclusion sample behaves like pure HTPB before cavitation (cycle 5) and like propellant after cavitation. Relaxation amplitudes can be associated to both mechanisms. Besides, Figure 10b shows that, for the first time, friction curve evolution is the closest to propellant, whereas cavitation and inclusion responses are similar to the linear one. This seems consistent with nonlinearities expresses by filled elastomers: after an unloading step, the reloading curve presents a stress softening, whereas after a relaxation step, the reloading curve presents a stress hardening; it seems realistic that these opposite behaviors come from different sources.

In regard to these results, the link between macroscopic nonlinearities and the two micomechanisms is clearer. Some effects can be attributed to friction, others to cavitation and some to both. This exploitation heightens some trends that are not obvious on the stress curves. The inclusion sample is particularly interesting; in most cases it presents the closest behavior to the propellant one, despite its very simple geometry. This possibly means that it gathers all the necessary elements to explain the macroscopic behavior of filled elastomers: linear viscoelasticity from the binder stress concentrations due to the inclusion presence, interface breakage leading to friction and cavitation.

Possible correlation between macroscopic nonlinearities and micromechanisms

According to the stress curves and post-processing analyses, an explanation of the macroscopic nonlinearities expressed by filled elastomers can be proposed. The idea is to associate one nonlinearity to one main mechanism. It is illustrated on Figure 11.

Voids nucleation and growth around the particles seem responsible for most of the stress softening phases occurring during monotonous and cyclic loads. Stress softening observed during reloading after an unloading step, and the underlying Mullins effect, are probably due to the fact that cavities are already open, so less energy is required to reach the same stress level. When the previous maximum is reached, pre-existing cavities are completely reopened and the curve meets the monotonous path. From this point, new cavities start to open. Also, because of the binder viscoelasticity, cavities still grow during relaxation steps, increasing stress drops.

Friction is more probably responsible for effects related to stress hardening. Stress curves

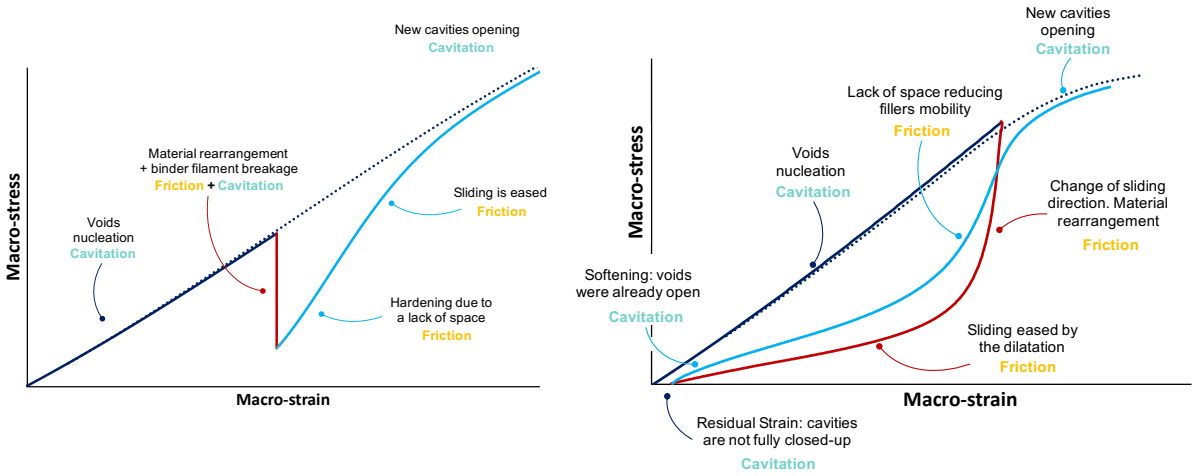

Figure 11: Possible correlation between macroscopic nonlinearities expressed by filled elastomers and involved micromechanisms.

from Figure 7 shows that friction leads to the convex unloading path, with a slope change. A possible explanation is that during loading steps, the microstructure organizes so that particles have more room to move. At the beginning of unloading, everything needs to rearrange and to move in the opposite direction, which obviously generates more friction. For the same reason, friction may amplify stress losses during relaxation steps, because the microstructure rearranges and stabilizes in a lowest entropy position. Stress hardening occurring after a relaxation step is due to the energy required to leave this lowest entropy position, as a strong friction opposes the movement.

DISCUSSION

Experiments reliability and reproductibility

As explained previously, samples are molded, which make them very reproductible. HTPB is quite easy to manipulate. Its viscosity is weak, which make experimental results very repeatable.

The hardest samples to manipulate are friction ones. If the alignment between the upper and lower end-plates is not perfectly ensured during bonding, a friction between the inner metallic bar and the upper end-plate can occur, interfering with the results. A particular

attention has been payed to this bonding step, and additional elements have been used to ensure alignment and avoid metal/metal friction.

Different ways can be used to calculate dissipated energies and reloading stiffness evolutions, all leading to similar conclusions. The method chosen is the one that provides the most understandable visual representation (see Appendix).

Scales and representativeness

Geometry of the samples may be questioned in regard to the real microstructure of filled elastomers. However, discarding the shape, size, volume ratio and nature of the particles is a voluntary choice. It is believed that a change of one of these parameters would only affect cavitation and friction rates, but not their effects. For instance, should the particles be bigger, more numerous, or ellipsoidal instead of spherical, only the contact area with the binder would be modified, leading to more or less friction, and more or less cavitation. Although geometry representativeness can be a perspective to this work, it is believed that general results and assertions would be the same.

Designing macroscopic samples was the only way to ensure a complete dissociation of the mechanisms. In real filled elastomers, at the particles scale, the binder acts as a homogeneous media. What is called micro-friction between the binder and the particles is equivalent to friction as defined in continuum mechanics. Similarly, voids created in filled elastomers microstructures are smaller than voids created in the macroscopic sample used here, but they are also more numerous; effects of several small cavities on the macroscopic response are considered to be equivalent to the ones of one large void.

The major difference between what happens in these macroscopic samples and what occurs in the real microstructure is probably related to interactions in filled elastomers; closeness of particles generates a strong coupling between the mechanisms. The nonlinearities explanation proposed previously remains hypothetical and simplified: assigning one nonlinearity to one main mechanism can be helpful in the development of new models.

CONCLUSIONS

A lack of information is encountered in literature regarding the direct effects of fundamental micromechanisms on the macroscopic behavior of filled elastomers. An experimental set up has been designed to evaluate friction and cavitation contributions to the macroscopic nonlinearities. Macroscopic samples made of HTPB, a linear viscoelastic, transparent, unfilled binder are used to study the mechanisms separately. The study shows that introducing friction and cavitation inside a material behaving linearly leads to the generation of specific nonlinearities. Comparison of stress, energy dissipation and reloading stiffness curves allows to compare the trends of the samples responses with a filled elastomer, here a solid propellant. The inclusion sample also provided rich information regarding the importance of the microscopic damage of the binder/filler interface. Similarities between nonlinearities expressed by this sample and by propellant suggest that friction and cavitation are enough to explain most of the macroscopic behavior. A correlation is made, showing that friction acts mostly during the hardening stress steps, whereas cavitation is responsible for nonlinearities related to stress softening. Each nonlinearity observed in filled elastomers behavior under loading-unloading and loading-relaxation is associated with a dominant micromechanism.

Although this study does not provide quantified information about the proportion of each mechanism acting at the microscale, it leads to a better insight of the material behavior. This can help the development of more physical models by suggesting consistent internal variables and evolutions laws. Results encourage the development of models accounting for both mechanisms, that seem to be equally important to explain the macroscopic nonlinearities.

ACKNOWLEDGMENTS

The authors would like to thank the Association Nationale de Recherche et Technologie (grant number 2016/1476), the Centre National de la Recherche Scientifique, ArianeGroup and CentraleSupelec for supporting and funding this research.

Nonlinearities presented by filled elastomers under uniaxial relaxation and unloading cycles

Figure 12 presents the typical responses of filled elastomers to unitary loading-unloading and loading-relaxation cycles. Nonlinearities are listed below:

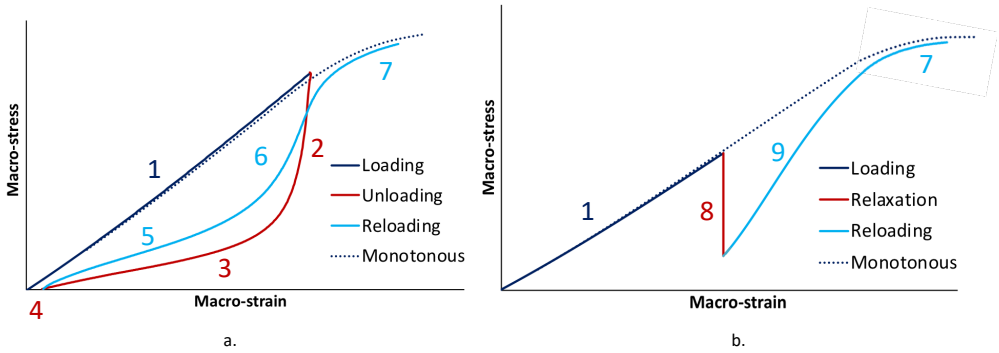

Figure 12: Nonlinear responses of highly filled elastomers under unloading (a) and relaxation (b) cyclic loads.

1. Monotonous loading curve is initially linear, before a stress softening occurs;
2. Stress decreases quickly for the first half of unloading, with a convex shape;
3. Stress decreases softly for the second part of unloading;
4. A residual strain remains when the stress vanishes;
5. A large stress softening occurs during reloading step until the previous maximum strain is reached (Mullins effect);
6. At the end of reloading, stress starts to harden and tends toward the monotonous loading curve;
7. Reloading curve catches up with monotonic curve when the stress reaches the previous maximum stress;
8. A large stress decrease occurs during relaxation;
9. A strong hardening occurs during the first part of reloading.

Dissipated energy and reloading stiffness calculation

To provide a deeper analysis of the stress curves from the HTPB samples tests, two quantities are used: dissipated energy at each cycle and evolution of the reloading stiffness of each cycle. Calculations are made using a Matlab code.

Dissipated energy corresponds to the hysteresis area of the stress-strain curves for loading-unloading$_1$ and loading-unloading$_5$ tests, and to the cycle area for loading-relaxation tests as indicated on Figure 13. Designated areas are calculated using the trapezoidal rule.

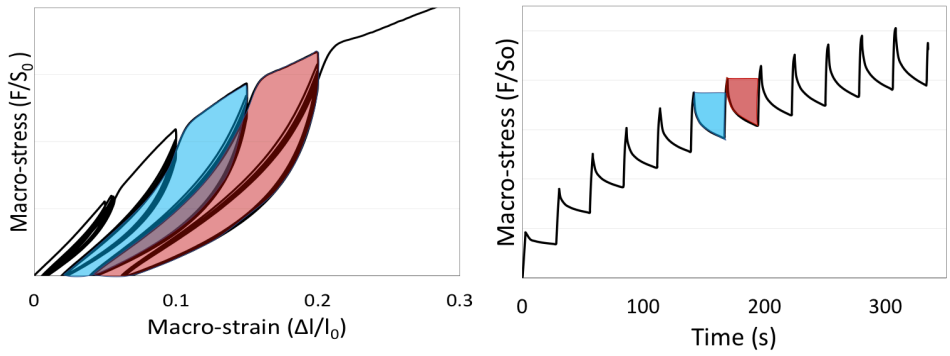

Figure 13: Area calculated to determine the energy dissipated during unloading (a), and relaxation (b) cycles.

To calculate the reloading stiffness (Figure 14), the stress-strain curves derivative is calculated for the first 2% of strain of each cycle. This quantity is then normalized by the first loading stiffness, measured on the first cycle.

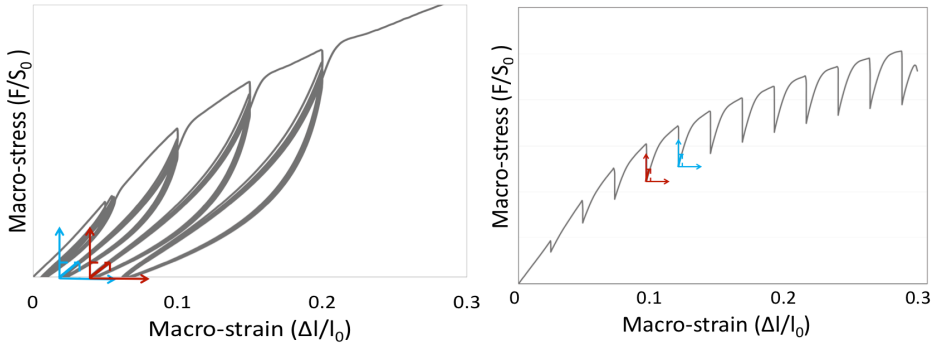

Figure 14: Coordinate systems used to calculate the reloading stiffness after each unloading (a) and relaxation (b) cycle.

References

1. A. Davenas. *Solid rocket propulsion technology.* Pergamon Press, 1993.

2. J. Diani, B. Fayolle, and P. Gilormini. A review on the mullins effect. *European Polymer Journal*, 45(3):601–612, 2009.

3. P. Gilormini ; N. Desgardin P-A. Toulemonde ; J. Diani. On the account of a cohesive interface for modeling the behavior until break of highly filled elastomers. *Mechanics and Materials*, 93:124–133, 2016.

4. A. Azoug, R. Nevière, R. Pradailles-Duval, and A. Constantinescu. Influence of fillers and bonding agents on the viscoelasticity of highly filled elastomers. *Journal of Applied Polymer Science*, 131(16):124–133, 2014.

5. G. Kraus, C. Childers, and K. Rollman. Stress softening in carbon black-reinforced vulcanizates. strain rates and temperature effects. *Journal of Applied Polymer Science*, 10:229–240, 1966.

6. A. Azoug, R. Nevière, R. Pradailles-Duval, and A. Constantinescu. Influence of crosslinking and plasticizing on the viscoelasticity of highly filled elastomers. *Journal of Applied Polymer Science*, 131(12), 2014.

7. N. Suzuki, M. Ito, and F. Yatsuyanagi. Effects of rubber/filler interactions on deformation behavior of silica filled sbr systems. *Polymer*, 46:193–201, 2005.

8. D. Hanson, M. Hawley, R. Houlton, K. Chitanvis, P. Rae, E. Orler, and D. Wrobleski. Stress softening experiments in silica-filled polydimethylsiloxane provide insight into a mechanism for the mullins effect. *Polymer*, 46(24):10989–10995, 2005.

9. H. Zhang, A. Scholz, J. de Crevoisier, F. Vion-Loisel, G. Besnard, A. Hexemer, H. Brown, E. Kramer, and C. Creton. Nanocavitation in carbon black filled styrene–butadiene rubber under tension detected by real time small angle x-ray scattering. *Macromolecules*, 45(3):1529–1543, 2012.

10. Z. Tao, S. Ping, Z. Mei, and Z. Cheng. Microstructure deformation and fracture mechanism of highly filled polymer composites under large tensile deformation. *12th International Symposium on Multiscale, Multifunctional and Functionaly Graded Materials, IOP Science.*, 2013.

11. F. Buech. Molecular basis for the mullins effect. *Journal of Applied Polymer Science*, 4:107–114, 1960.

12. G. Marckmann, E. Verron, L. Gornet, G. Chagnon, P. Charrier, and P. Fort. A theory of network alteration for the mullins effect. *Journal of the Mechanics and Physics of Solids*, 50(9):2011–2028, 2002.

13. J. Bergström and M. Boyce. Constitutive modeling of the large strain time-dependant behavior of elastomers. *Journal of Mechanics and Physics of Solids*, 46:931–954, 1998.

14. F. Hild, A. Fanget, J. Adrien, E. Maire, and S. Roux. Three dimensionnal analysis of a tensile test on a propellant with digital volume correlation. *Archives of Mechanics*, 63(5), 2011.

15. J. Grancoin, A. Boukamel, and S. Lejeunes. A micro-mechanically based continuum damage model for fatigue life prediction of filled rubbers. *International journal of Solid and Structures*, 51(6):1274–1286, 2014.

16. R. Schapery. A micromechanical model for non-linear viscoelastic behavior of particle-reinforced rubber with distributed damage. *Engineering Fracture Mechanics*, 25(5):845 – 867, 1986.

17. A. Sudar, J. Moczo, G. Vörös, and B. Pukanszky. The mechanism and kinetics of void formation and growth in particulate filled pe composites. *eXPRESS Polymer Letters*, 1(11):763–772, 2007.

18. S. Ozupeck and E. Becker. Constitutive equations for solid propellants. *Journal of Engineering Materials and Technology*, 119:125–132, 1997.

19. International Rubber Conference. *A new modelling of the Mullins' effect and viscoelasticity of elastomers based on physical approach*, 2002.

20. S. Cantournet, R. Desmorat, and J. Besson. Mullins effect and cyclic stress softening of filled elastomers by internal sliding and friction thermodynamics model. *International Journal of Solids and Structures*, 46(11-12):2255–2264, 2009.

21. H. Lorenz, J. Meier, and M. Klüppel. Micromechanics of internal friction of filler reinforced elastomers. In *Elastomere Friction*, pages 27–52. Springer, 2010.

22. M. Kaliske and H. Rothert. Constitutive approach to rate-independent properties of filled elastomers. *International Journal of Solids and Structures*, 35(17):2057 – 2071, 1998.

23. A. Azoug, A. Constantinescu, and R. Nevière. Microstructure and deformation mechanisms of a solid propellant using 1h nmr spectroscopy. *Fuel*, 148:39–47, 2015.

24. A. Hamdi, S. Guessasma, and M. Abdelaziz. Fracture of elastomers by cavitation. *Material and Design*, 53:497–503, 2014.

25. A. Oberth and R. Bruenner. Tear phenomena around solid inclusions in castable elastomers. *Transactions of the Society of Rheology*, 9(2):165–185, 1965.